

MEASUREMENTS OF SPACE CHARGE AND FINITE GEOMETRY EFFECTS ON EMITTANCE IN THE UNIVERSITY OF MARYLAND HIGH PERVEANCE ELECTRON GUN†

D. KEHNE and M. REISER

*Laboratory for Plasma Research and Department of Electrical Engineering, University
of Maryland, College Park, Maryland 20742.*

(Received 3 December 1990)

Experimental emittance measurements of the University of Maryland high perveance electron gun have been performed. Measurements were accomplished using the slit/pinhole technique. Despite the presence of substantial space charge expansion in the sampled beamlets, an accurate value of emittance is achieved by using slits of different sizes and extrapolating the slit width to zero. Attempted elimination of this space charge error by simulation produces only partial success. Finite geometry effects are shown to be negligible.

1 INTRODUCTION

Emittance measurements of beams with the high current densities and low emittances associated with heavy ion inertial fusion suffer from errors generated by the space charge expansion of the sampled beamlets. This error compounds the inherent finite geometry errors present in all sampling emittance meters. Measurements of the source emittance of the University of Maryland 5-kV, 245-mA electron gun (a 5:1 scaled-down version of the SLAC klystron gun) have been performed via the slit/pinhole technique. The 12.7 mm radius thermionic cathode ($kT = 0.115$ eV) generates a converging beam, which has a waist of radius 6.1 mm approximately 8 mm past the gun exit (anode).

A diagnostic chamber was constructed for measuring gun characteristics. Diagnostics include a moveable phosphor screen (for examining beam expansion) and an emittance meter. Four vertical slits of widths 0.258 mm, 0.204 mm, 0.138 mm, and 0.055 mm, each with 0.005 mm accuracy, are located 45 mm from the anode. Also located at the slit position is a pinhole/charge collector used for measuring the current density profile. A plot of the normalized current density of the 5-kV, 245-mA full beam at the slit location is shown in Figure 1. The beam profile is distinctly hollow, which is attributed to the nonlinear electrostatic forces in the A–K gap region. A horizontally sweeping charge collector (consisting of a pinhole of radius $r_p = 0.1$ mm and a Faraday cup) mounted 135 mm from the anode (85 mm from the slits) allows the emittance to be measured via the slit/pinhole method. The slits are constructed

† Research supported by the U.S. Department of Energy

Normalized Current Density vs Beam Radius

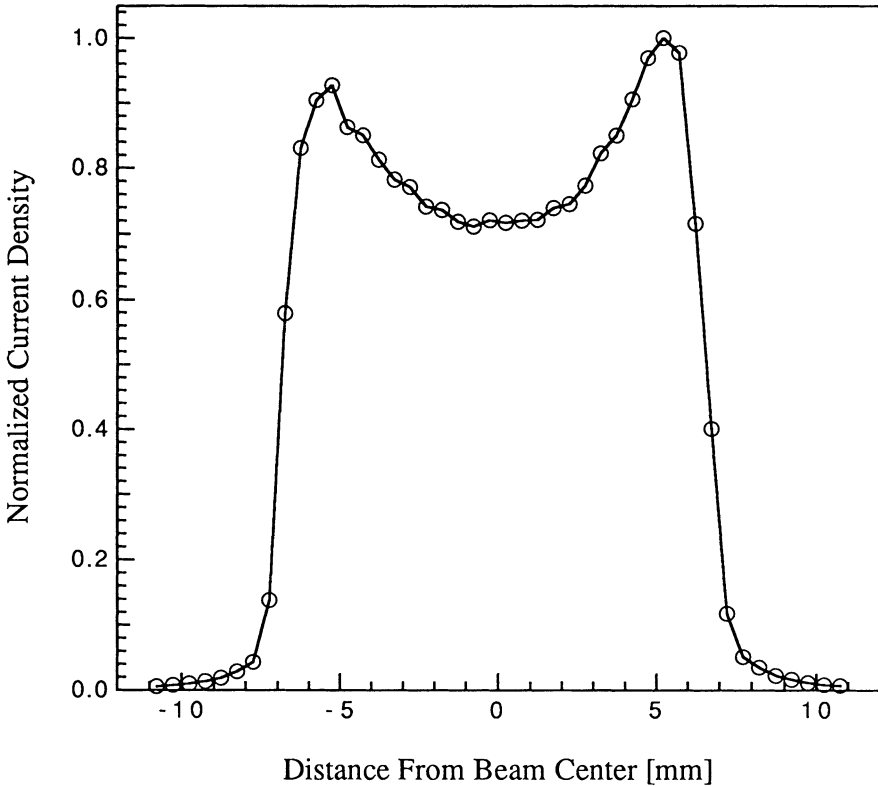


FIGURE 1 Normalized current density profile of full 245-mA, 5-kV beam taken 45 mm from anode with a pinhole/Faraday cup assembly.

from 0.05-mm-thick tantalum foil. The pinhole/cup assembly is mounted on an XYZ, manipulator which positions the cup to 0.02 mm accuracy. Figure 2 shows, in schematic form, a beam profile measured with the pinhole/Faraday cup when the slit is located at a distance x_s from the beam axis and the distribution is Gaussian in transverse angles $x' = \xi/L$. The mean angle η is defined by the peak of the curve while the rms width of the distribution is measured by the parameter σ as shown in the figure. The normalized current density is represented by $n(r)$. The functions $\sigma(r)$, $\eta(r)$, and $n(r)$ are determined from the individual beam profiles. Following Rhee and Schneider¹, the beam density distribution function $f_4(x, x', y, y')$ in 4-dimensional trace space can be written

$$f_4 = \frac{n(r)}{(2\pi)^{1/2}\sigma(r)} \exp\left(\frac{-(x' - \eta(r)x/r)^2 - (y' - \eta(r)y/r)^2}{2\sigma^2(r)}\right). \quad (1)$$

By numerically integrating $f_4(x, x', y, y')$ over y and y' , we can calculate the rms quantities $\langle x^2 \rangle$, $\langle x'^2 \rangle$, and $\langle xx' \rangle^2$ and hence the effective emittance of the beam,

EMITTANCE MEASUREMENT: SLIT/PINHOLE METHOD

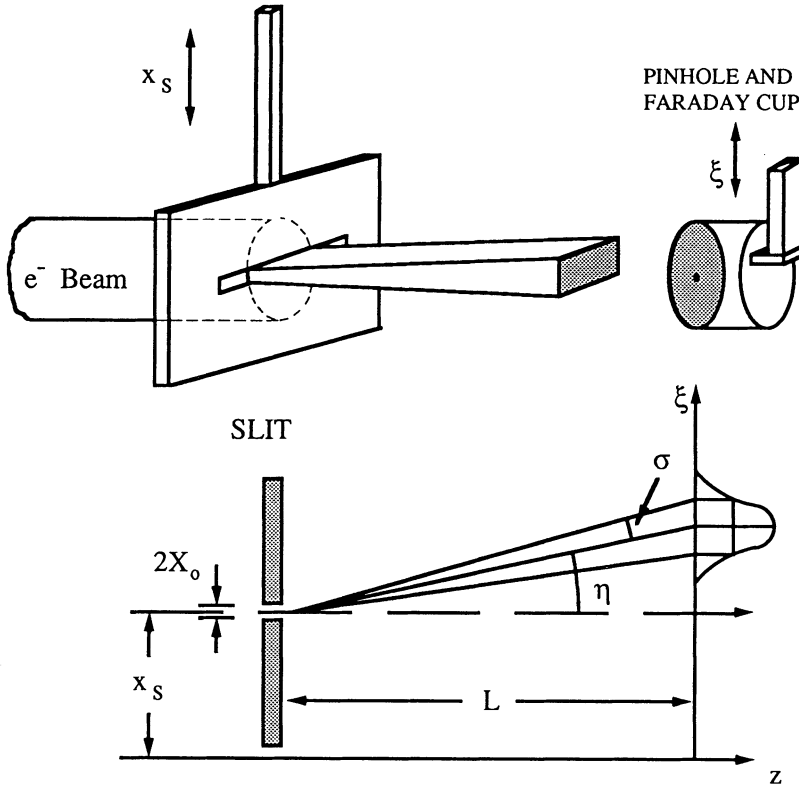


FIGURE 2 Schematic of the slit/pinhole system. The slit masks out a sheet beam and the pinhole/Faraday cup samples across its width.

which is defined as

$$\varepsilon = 4\varepsilon_{\text{rms}} = 4(\langle x^2 \rangle \langle x'^2 \rangle - \langle xx' \rangle^2)^{1/2}. \tag{2}$$

This analysis assumes that space-charge and finite-geometry effects are negligible in the expansion of the sheet beamlets. If these sources of error are small, each slit measurement should result in the same emittance value. If they are significant, the zero slit width emittance can be extrapolated from the data². In Figure 3, the measured emittances are plotted versus slit width, along with a best linear fit to the points. In addition, values of emittance compensated for space charge and finite geometry errors are shown; they will be discussed later. The nonuniformity of the measurements suggests that a slit-width-dependent error is present. Determining which error is dominant is fairly straightforward, and subsequent analysis can partially compensate for these effects. Note, however, that the most reliable value of the emittance is extrapolated from the data. In this case, the extrapolated emittance is 97 mm-mrad. This corresponds to a growth of 1.13 over the intrinsic thermal

Emittance vs Slit Width

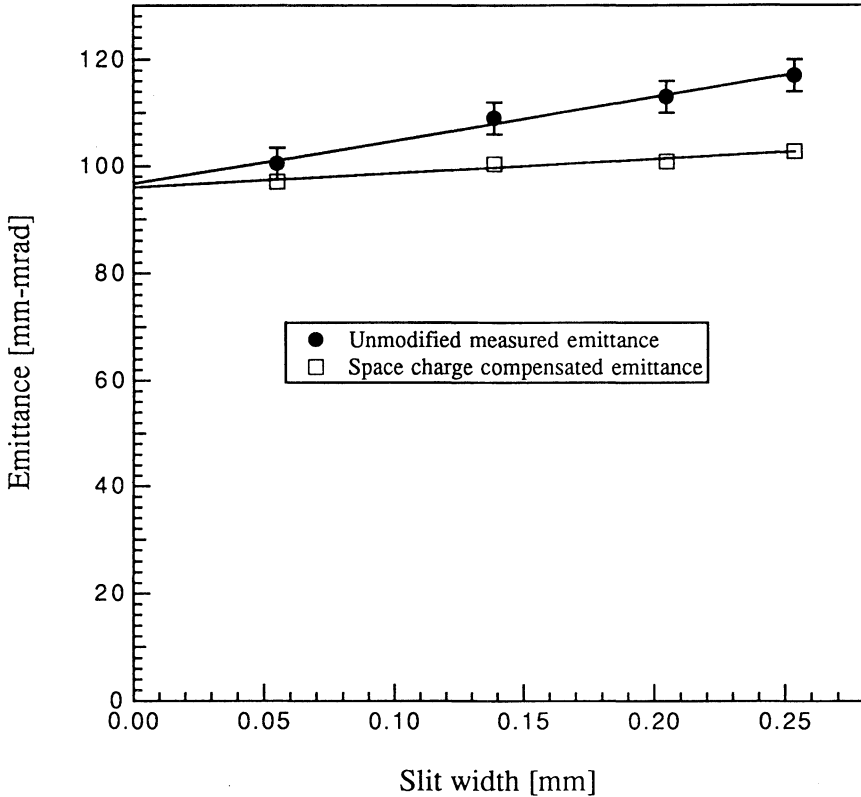


FIGURE 3 Plot of emittance vs. slit width for the measured values and the space charge compensated values using the 1-dimensional sheet beam model. Also shown are the best linear fits to each.

emittance defined by $\varepsilon_{\text{int}} = R_c(2kT_c/qV_0)^{1/2} = 86 \text{ mm-mrad}$. Here R_c is the cathode radius, k is Boltzmann's constant, T_c is the temperature of the cathode, q is the charge of an electron, and V_0 is the accelerating voltage. These values of emittance, as well as all other values of emittance discussed in this paper, are unnormalized.

2 FINITE SLIT EFFECT

The slit/pinhole technique and data analysis described earlier assumes that the expansion of each beamlet between the slit and pinhole depends only on the velocity distribution of the particles. In a well-designed emittance meter, this is a good approximation. However, unavoidable errors are introduced by the finite size of the slit and pinhole. In addition, a finite-size sheet beam also has a finite current. This space charge causes additional expansion over that due to emittance. Thus, the measured distribution at the pinhole depends not only on the velocity distribution,

but on the slit width, pinhole size, and the current density of the sheet beam. These three sources of error can be analyzed by using an appropriate beam model.

The model we use is the 1-dimensional beam envelope equation. The differential equation describing the full beam envelope X_m is

$$X_m'' - qJ_0/(m\epsilon_0(\beta\gamma)^3) - \epsilon_x^2/X_m^3 = 0, \quad (3)$$

where J_0 is the current density of the sheet beam, m is the electron mass, ϵ_0 is the permittivity of free space, c is the speed of light, γ is the relativistic mass factor, and $\beta = 1 - 1/\gamma^2$. The emittance of the full beam ϵ_x is defined by $X_0(3kT_s/2qV_0)^{1/2}$, where X_0 is the half slit width and T_s is the temperature of the beam at the slit. This model incorrectly characterizes the initial beam as an infinite sheet, but this assumption is fairly good even near the beam edge where the ratio of X_0 to the long axis of the actual sheet beam is no less than 1/10. This equation has analytic solutions when either the current or emittance is zero.

One estimate³ of the finite-slit effect calculates the phase-space area that results when a zero-emittance beam is measured by a finite slit and ideal detector. In a nonzero emittance beam, this finite slit emittance value would be subtracted from the measured emittance to give a lower limit on the emittance. In our case, this approximation overestimates the effect of the finite slit. We use the sheet beam analysis to better estimate this error. Since the slit samples upright sections of the phase space of the full beam, the initial envelope slope X_0' is assumed to be zero. If space charge is equal to zero, the 1-dimensional sheet beam equation has the solution

$$X_m(L) = (X_0^2 + 3L^2kT_s/2qV_0)^{1/2}, \quad (4)$$

where L is the slit/pinhole separation. In order to estimate this effect, the value for temperature T_s in this equation can be approximated using the experimentally extrapolated emittance and the equation $\epsilon_x = R_{\text{rms}}(4kT_s/eV_0)^{1/2} = 97 \text{ mm-mad}$. Using the profile in Figure 2, the rms radius of the full beam, R_{rms} , is calculated numerically to be 4.85 mm. R_{rms} relates to the full beam radius R according to $(R_{\text{rms}})^2 = R^2/2$. The subsequent value for T_s is 0.496 eV. For slits widths of 0.055 mm, 0.138 mm, 0.204 mm and 0.258 mm, the percent increase in the envelope at the pinhole due to finite slit effects are respectively 0.04%, 0.2%, 0.5%, and 0.8%, which are negligibly small.

A more accurate method of predicting the finite-slit effect is to perform a superposition of point sources, each with a given velocity distribution, over the slit⁴. From this, the actual final beam density as a function of its width can be calculated. Assuming a Maxwellian velocity distribution with rms half width of σ at the slit and uniform density n_0 across the slit, the density distribution $n(x)$ at the pinhole plane is

$$n(x) = \frac{n_0}{2} \left[\text{erf}\left(\frac{|x| + X_0}{\sqrt{2}\sigma L}\right) - \text{erf}\left(\frac{|x| - X_0}{\sqrt{2}\sigma L}\right) \right], \quad (5)$$

where the error function is defined by

$$\text{erf}(u) = (2/\pi^{1/2}) \int_0^u \exp(-t^2) dt. \quad (6)$$

Using the equation¹ $\sigma^2 = kT_s/(m\beta^2c^2)$ and $T_s = 0.496$ eV to derive an approximate value of σ , the percent increases in the rms width of the 0.055-mm, 0.138-mm, 0.204-mm, and 0.258 mm slits are respectively 0.03%, 0.2%, 0.5% and 0.7%. These numbers are essentially the same as those determined by the sheet model. In both cases it is evident that the finite-slit effect is essentially negligible in these emittance measurements.

3 FINITE PINHOLE EFFECT

Another source of geometrical error is caused by the finite size of the pinhole/Faraday cup detector. As in the case of a finite slit, the finite-pinhole effect can be estimated³ by assuming that an infinitely thin sheet beamlet of zero emittance is scanned by a pinhole of finite diameter. A finite phase space area results and this value is subtracted from the measured emittance to obtain a lower limit on emittance. Again, this is not an accurate estimate in this experiment. In our case, the pinhole is small (1/10) of the rms width of the narrowest profile with respect to the expanded sheet beamlets. Furthermore, the profiles being measured have no sharp density gradients. Thus, the pinhole provides an accurate averaging process over a nearly linear range of the distribution being measured. The pinhole effect can be calculated fairly accurately by determining the current passing through the pinhole at a certain location when the beam has a Gaussian distribution in space (very nearly true in this case). Doing this for every pinhole location produces a density profile. Fitting this profile to a Gaussian reveals an increase in rms width of approximately 0.1% over the range of measured values of gaussian rms width σ . Thus, the finite pinhole has negligible contribution to the measured values of emittance.

4 COMPENSATION FOR SPACE CHARGE

Space charge expansion of the sheet beamlets is another source of error that can cause the measured error to be too large. Compensation for space charge in the sheet beamlets is accomplished using the 1-dimensional sheet beam model. To do this, it is necessary to make several assumptions. The current density must be derived from the normalized current density profile in Figure 2. Since this sheet beam model assumes uniform current density and the profile is measured across the center of the beam, the current density at the beamlet center is used in the simulations. Since the actual beamlets are not uniform, this is a possible source of error. The temperature of the beam used to calculate the simulated sheet beam emittance is estimated in the following way.

The temperature of the simulated beamlet is varied until its rms width at the detector plane is equal to the rms width of the measured sheet beamlet. The simulation is again run with the space charge term set to zero. The resultant rms width of the simulated beamlet at the pinhole plane is the modified rms width σ for the profile at that slit location. This is done for each slit location. The modified values for σ are

then used in the analysis described earlier. The results of the modification are shown in Figure 3. If the compensation was perfect, the values of the modified emittances would be identical. This is obviously not the case and has several possible explanations.

First, this model is not exact. It assumes uniform density of the sheet beamlets. Though this is true over the widths of most of the beams, the density gradient becomes substantial at the beam edge. In addition, the sheet beamlets are not uniform along their lengths. This model uses the current density at the point where the pinhole sweeps across the sheet beam. In the experiment, when the slit is sampling near the center of the full beam, regions of high current density surround the lower-current density region at the sheet beam center. As the sheet beam propagates, the regions of higher current density will flow into the regions of lower current density. This causes an increase in the measured width of the sheet beamlets that is not present in the simulated beamlets. With regard to the experimental apparatus, there might be an effect that has not been taken into account, such as secondary emission of the slit plate or aperture lensing of the slit, that is causing the beamlets to diverge more than they should. All of these possibilities are being explored.

REFERENCES

1. M. J. Rhee and R. F. Schneider, *Part. Accel.* **20**, 133 (1986).
2. J. Guyard and M. Weiss, *Proc. Proton Linear Accel. Conf.*, Chalk River, 1976, rep. AECL 5677, p. 254.
3. C. Lejeune and J. Aubert, "Emittance and Brightness: Definitions and Measurements", *Applied Charged Particle Optics: Advances in Electronics and Electron Physics, Supplement 13A*. Edited by A. Septier, Academic Press Inc. 1980, New York.
4. W. Namkung and E. P. Chojnacki, *Rev. Sci. Instrum.* **57**, 341 (1986).